

Diffractive electroproduction of heavy quarkonia: Spin rotation effects for the photon-like transition $V \rightarrow Q\bar{Q}$

Michal Krelina^{1,2,*}, Jan Nemchik^{2,3,†} and Roman Pasechnik^{4,5,6‡}

¹*Departamento de Física, Universidad Técnica Federico
Santa María, Casilla 110-V, Valparaíso, Chile*

²*Czech Technical University in Prague, FNSPE,
Břehová 7, 11519 Prague, Czech Republic*

³*Institute of Experimental Physics SAS,
Watsonova 47, 04001 Košice, Slovakia*

⁴*Department of Astronomy and Theoretical Physics,
Lund University, SE-223 62 Lund, Sweden*

⁵*Nuclear Physics Institute ASCR, 25068 Řež, Czech Republic*

⁶*Departamento de Física, CFM, Universidade Federal de Santa Catarina,
C.P. 476, CEP 88.040-900, Florianópolis, SC, Brazil*

Abstract

The strong onset of spin effects is usually ignored interpreting the dynamics of diffractive electroproduction of heavy quarkonia. We present for the first time the study of the Melosh spin rotation in production of S -wave states off a nucleon target assuming a similar structure of the virtual photon $\gamma^* \rightarrow Q\bar{Q}$ and vector meson $V \rightarrow Q\bar{Q}$ transitions. We employ the color dipole Light-Front formulation based upon the radial wave function of heavy quarkonia computed in the $Q\bar{Q}$ -pair rest frame by solving the Schrödinger equation with two realistic $Q\bar{Q}$ interaction potentials. Adopting the photon-like Lorentz structure of the $V \rightarrow Q\bar{Q}$ Light-Front wave function, we have found a significant reduction of the $J/\psi(1S)$ photoproduction cross section compared to experimental data due to the Melosh transformation. We have also analysed the dependence of such a pronounced impact of spin effects on the photon energy and virtuality Q^2 , as well as on the quarkonia mass M_V . We have found their stronger onset in production of radially excited $2S$ and $3S$ states giving rise to a worse description of available data on the $\psi'(2S)$ -to- $J/\psi(1S)$ ratio of photoproduction cross sections. We conclude that many of recent studies of heavy quarkonia based on an unjustified assumption of a photon-like vector-meson $V \rightarrow Q\bar{Q}$ wave function and ignoring the Melosh spin rotation effects should be treated with a great caution and, consequently, cannot provide reliable predictions.

PACS numbers: 14.40.Pq,13.60.Le,13.60.-r

*Electronic address: michal.krelina@usm.cl

†Electronic address: nemcik@saske.sk

‡Electronic address: roman.pasechnik@thep.lu.se

I. INTRODUCTION

Elastic virtual photo- and electroproduction of heavy quarkonia $\gamma^* p \rightarrow J/\psi(\psi', \Upsilon, \Upsilon', \dots) p$ remains one of the most active fundamental research areas of Quantum Chromo Dynamics (QCD). These processes provide a very powerful tool for studies of various QCD phenomena in the framework of perturbative QCD (pQCD) since the length scale associated with heavy quarkonia is relatively small. This fact allows to minimize the underlined QCD uncertainties due to nonperturbative interactions (see Refs. [1, 2], while a comprehensive review on quarkonia phenomenology can be found in e.g. Refs. [3–5]). On the other hand, in nucleus-nucleus collisions the heavy charmonia and bottomonia production processes represent an important probe for the hot medium that emerges in heavy-ion collisions (see Ref. [6], for example).

The powerful method for probing the pQCD contribution to the quarkonium production amplitude is based on the so-called *scanning phenomenon* [7–12]. This phenomenon has been previously studied in detail in Ref. [1] in the case of the photo- and electroproduction of heavy quarkonia. Here, the corresponding production amplitude is scanned at dipole sizes $r \sim r_S$, where the scanning radius r_S defined as follows

$$r_S \approx \frac{3}{\varepsilon} = \frac{Y}{2\sqrt{Q^2 z(1-z) + m_Q^2}} \sim \frac{Y}{\sqrt{Q^2 + M_V^2}}. \quad (1.1)$$

Here, M_V is the mass of a heavy quarkonium state V , m_Q is the heavy quark mass, Q^2 is the photon virtuality, and z is the longitudinal momentum fraction of the photon taken by a (anti)quark in the photon leading-order Fock $\gamma^* \rightarrow Q\bar{Q}$ fluctuation. The latter represents a dipole of transverse separation \vec{r} . The factor $Y \sim 6$ in the nonrelativistic limit ($z \sim 1/2$, $M_V \sim 2m_Q$) as was previously found in Refs. [1, 9].

According to the scanning phenomenon, the onset of pQCD is reached at the sufficiently small value of $r_S \lesssim r_0$, in terms of $r_0 \sim 0.3$ fm which is the so-called the gluon propagation radius [13, 14]. In the case of heavy quarkonia production, this provides the relation [1, 12],

$$(Q^2 + M_V^2) \gtrsim Q_{\text{pQCD}}^2 = \frac{Y^2}{r_0^2}. \quad (1.2)$$

Such a condition is satisfied only for the photo- and electroproduction of bottomonia. However, in the case of charmonium production one requires rather large photon virtualities, typically $Q^2 \gtrsim 10 \div 20 \text{ GeV}^2$, in order to probe the pQCD regime. Another manifestation of the scanning phenomenon is based on the universality properties in production of different heavy quarkonium states as a function of the scaling variable $Q^2 + M_V^2$ [1, 9, 10, 12].

So, indeed the elastic electroproduction of heavy quarkonia at $Q^2 \gg 0$ is an efficient tool for studying the QCD phenomena by probing mainly the hard QCD scale, thus, enabling us to minimize the theoretical uncertainties and to safely rely on the pQCD approach in the analysis of the corresponding observables [2]. Only electroproduction of charmonia at small $Q^2 \lesssim M_V^2$ (see Eq. (1.2)) explores the semihard-scale physics of mainly a nonperturbative origin.

Consequently, the quarkonia electroproduction reactions have been adopted in Refs. [1, 2] for a detailed analysis of the *Melosh spin rotation* effects [15] within the color dipole formalism [7–10, 16–20]. We have found for the first time a strong onset of these effects

significantly modifying the quarkonium production cross sections, especially for radially-excited $2S$ and $3S$ production. This is a very relevant result provided that the Melosh spin transformation has been continuously ignored almost in all earlier publications devoted to electroproduction of heavy quarkonia (see Refs. [1, 2] and references therein).

The analysis of spin effects in our previous studies [1, 2] has been performed assuming that the Light-Front (LF) wave functions of $Q\bar{Q}$ fluctuation for the vector meson and for the virtual photon states have a different structure¹. This has been justified by the fact that in the case of charmonium production a photon-like structure of LF quarkonium wave function leads to an appearance of both S - and D -wave states in the radial wave function in the $c\bar{c}$ rest frame. Consequently, the weight of the D -wave state is strongly correlated with the structure of the charmonium vertex and cannot be understood in the framework of any realistic nonrelativistic $c - \bar{c}$ interaction potential. For the first thorough discussion of elastic electroproduction of the D -wave states, see Ref. [22].

Despite of this fact, practically all publications existing in the literature devoted to charmonium electroproduction (see Ref. [2] and references therein) are based on an unjustified assumption of a similar Lorentz structure for the photon and vector meson vertices. Moreover, the corresponding calculations of electroproduction cross sections found in the literature have been performed totally ignoring the effects of Melosh spin transformation between the $Q\bar{Q}$ rest frame and the LF (infinite-momentum) frame. For this reason, in the present paper we analyze for the first time a modification of quarkonium production yields caused by such spin effects and derive the corresponding formulas for electroproduction cross sections. Our current predictions with a photon-like structure of the quarkonium vertex are compared with our previous results [1, 2] based on a different structure of both $\gamma^* \rightarrow Q\bar{Q}$ and $V \rightarrow Q\bar{Q}$ transitions. As the main result, we find a strong correlation between the onset of spin effects and the structure of the distribution amplitude of $Q\bar{Q}$ fluctuation for the heavy quarkonium.

In the next Sec. II, we present a short review of the factorized color dipole formalism and its application to elastic heavy quarkonia photo- and electroproduction. We specify shortly the relevant ingredients of the forward production amplitudes, such as the LF wave function for a transversely and longitudinally polarized virtual photon and heavy quarkonia, as well as the flavor-independent universal dipole cross section depending on the collisions energy and on the transverse separation between Q and \bar{Q} . Here, we impose the same Lorentz structure for the photon and heavy quarkonium distribution amplitudes of their lowest $Q\bar{Q}$ Fock fluctuations following the conventional approach in the literature. On top of that, we incorporate also the Melosh spin transformation and obtain for the first time the final full expressions for electroproduction amplitudes in the LF frame.

The next Sec. III is devoted to comparison of our model parameter-free calculations with available data for $J/\psi(1S)$ and $\Upsilon(1S)$ photoproduction assuming the same Lorentz structure of both the photon and quarkonium wave functions. We have found a reasonable agreement with data excluding the spin rotation effects following the standard approach adopted in the literature. However, the inclusion of the Melosh spin transformation leads to a counter-intuitive reduction of the electroproduction cross section thus spoiling such a good description of data. Here, we compare our calculations with our previous results based on a different S -wave structure for the $V \rightarrow Q\bar{Q}$ wave function compared to that of the

¹ The LF wave-function formalism accounting for the Melosh spin transformation has been recently applied in studies of $\gamma^*\gamma^* \rightarrow \eta_c(1S), \eta_c(2S)$ transition form factor in Ref. [21]

photon. In this case, on the contrary, the spin effects lead to a desired enhancement of the quarkonium electroproduction cross section significantly improving its agreement with available data. Thus, we have found a strong correlation between the onset of the spin rotation effects and the Lorentz structure of the quarkonium vertex. We also demonstrate that, in comparison with $1S$ state, the onset of the spin effects appears to be stronger in production of the radially-excited $2S$ and $3S$ states as an implication of a nodal structure in the corresponding radial wave functions. This implies a stronger reduction of corresponding electroproduction cross sections hence providing a worse description of available data e.g. on the $\psi'(2S)$ -to- $J/\psi(1S)$ ratio of charmonium yields.

Finally, in Sec. IV we summarise the results obtained in our study.

II. AN OVERVIEW OF THE COLOR-DIPOLE APPROACH TO ELECTROPRODUCTION OF HEAVY QUARKONIA

In the present paper, we treat the photo- and electroproduction of S -wave heavy quarkonium states in the framework of color dipole approach [1, 2, 7–10, 16, 18]. In the target rest frame the projectile photon (real, with $Q^2 \rightarrow 0$, or virtual) undergoes strong interactions via its Fock components with the target. Here, the lowest state in the Fock state expansion for the relativistic vector meson is represented by the quark-antiquark $Q\bar{Q}$ pair. Such a state can be considered as a color dipole whose scattering depends on the transverse separation between the quark and antiquark and on the light-cone (LC) momentum fraction of the meson taken by a heavy (anti)quark. Consequently, the dipole interactions with a target is described by the dipole cross section $\sigma_{Q\bar{Q}}$ (introduced for the first time in Ref. [23]), which is a flavor-independent universal function of the dipole separation and the Bjorken x (or the dipole-target scattering energy). Here, in the leading-log($1/x$) approximation the energy dependence of the dipole cross section emerges due to the presence of the higher Fock states with radiated gluons, for example, $Q\bar{Q} + g$ etc.

We start with the expression for the elastic electroproduction amplitude in the forward limit in the rest frame of the target [7–10, 16, 18],

$$\text{Im } \mathcal{A}_{T,L}^{\gamma^* p \rightarrow V p}(x, Q^2) = \int d^2r \int_0^1 dz \Phi_{V_{T,L}}^\dagger(r, z) \Psi_{\gamma_{T,L}^*}(r, z; Q^2) \sigma_{Q\bar{Q}}(x, r). \quad (2.1)$$

Here, the function $\Psi_{\gamma_{T,L}^*}(r, z; Q^2)$ is the LF wave function of the photon with virtuality Q^2 and with a transverse (T) or longitudinal (L) polarisation corresponding to its Fock $Q\bar{Q}$ component; \vec{r} represents the two-dimensional transverse separation within the $Q\bar{Q}$ -dipole; the variable $z = p_Q^+/p_\gamma^+$ is the boost-invariant fraction of the photon momentum carried by a heavy quark (or antiquark); $\Phi_{V_{T,L}}(r, z)$ is the LF vector meson wave function for T and L polarized heavy quarkonia sharing exactly the same LC variables with the photon wave functions; $\sigma_{Q\bar{Q}}(x, r)$ describes an interaction of the $Q\bar{Q}$ dipole (with transverse separation $r \equiv |\vec{r}|$) with the target, where $x = (M_V^2 + Q^2)/s$ which coincides with the standard Bjorken variable at large $Q^2 \gg M_V^2$, with the c.m. energy squared s of the electron-proton system (for more details, see Ref. [24]). One safely employs the nonrelativistic QCD (NRQCD) limit in studies of heavy quarkonia production in the relevant (measured) kinematical domains. In the computation of the total electroproduction $\gamma^* p \rightarrow V p$ cross section, we follow Ref. [18],

such that

$$\sigma^{\gamma^* p \rightarrow Vp}(x, Q^2) = \sigma_T^{\gamma^* p \rightarrow Vp} + \tilde{\varepsilon} \sigma_L^{\gamma^* p \rightarrow Vp} = \frac{1}{16\pi B} \left(\left| \mathcal{A}_T^{\gamma^* p \rightarrow Vp} \right|^2 + \tilde{\varepsilon} \left| \mathcal{A}_L^{\gamma^* p \rightarrow Vp} \right|^2 \right). \quad (2.2)$$

Here, $B = 4.73 \text{ GeV}^{-2}$ is the slope parameter and $\tilde{\varepsilon} = 0.99$ represents the photon polarization (used also in Refs. [1, 2]), both are independent of spin effects and are obtained by fitting to the H1 data at HERA [25]. The real part corrections are usually incorporated into the corresponding amplitudes $\mathcal{A}_{T,L}$ as follows [10, 26, 27],

$$\mathcal{A}_{T,L}^{\gamma^* p \rightarrow Vp}(x, Q^2) = \text{Im} \mathcal{A}_{T,L}^{\gamma^* p \rightarrow Vp}(x, Q^2) \left(1 - i \frac{\pi}{2} \frac{\partial \ln \text{Im} \mathcal{A}_{T,L}^{\gamma^* p \rightarrow Vp}(x, Q^2)}{\partial \ln x} \right). \quad (2.3)$$

The LF photon wave function, corresponding to the perturbative (leading-order) Fock $\gamma_{L,T}^* \rightarrow Q\bar{Q}$ fluctuations reads [28–30],

$$\Psi_{\gamma_{T,L}^*}^{(\mu, \bar{\mu})}(r, z; Q^2) = \frac{\sqrt{N_c \alpha_{\text{em}}}}{2\pi} Z_Q \chi_Q^{\mu\dagger} \hat{\mathcal{O}}_{\gamma^*}^{T,L} \tilde{\chi}_Q^{\bar{\mu}} K_0(\varepsilon r). \quad (2.4)$$

As usual, here we denote the number of QCD colors, $N_c = 3$, charge of the heavy quark, Z_Q (for the relevant cases considered in this work, $Z_c = 2/3$ and $Z_b = 1/3$, for the charm and bottom quarks, respectively), $\varepsilon^2 = z(1-z)Q^2 + m_Q^2$, the modified Bessel function of the second kind, $K_0(\varepsilon r)$, while the two-component (anti)quark spinors in the LF frame χ_Q^μ and $\tilde{\chi}_Q^{\bar{\mu}} \equiv i\sigma_y \chi_Q^{\bar{\mu}*}$ normalized as (see e.g. Ref. [31])

$$\sum_{\mu, \bar{\mu}} \left(\chi_Q^{\mu\dagger} \hat{A} \tilde{\chi}_Q^{\bar{\mu}} \right)^* \left(\chi_Q^{\mu\dagger} \hat{B} \tilde{\chi}_Q^{\bar{\mu}} \right) = \text{Tr}(\hat{A}^\dagger \hat{B}). \quad (2.5)$$

Besides, in Eq. (2.4) we introduce the operators in the spinor space denoted as $\hat{\mathcal{O}}_{\gamma^*}^{T,L}$ which are represented in the form

$$\begin{aligned} \hat{\mathcal{O}}_{\gamma^*}^T &= m_Q \vec{\sigma} \cdot \vec{e}_\gamma + i(1-2z)(\vec{\sigma} \cdot \vec{n})(\vec{e}_\gamma \cdot \vec{\nabla}_r) + (\vec{n} \times \vec{e}_\gamma) \cdot \vec{\nabla}_r, \\ \hat{\mathcal{O}}_{\gamma^*}^L &= 2Qz(1-z)\vec{\sigma} \cdot \vec{n}, \quad \vec{\sigma} = (\sigma_x, \sigma_y, \sigma_z), \quad \vec{\nabla}_r \equiv \partial/\partial \vec{r}, \end{aligned} \quad (2.6)$$

written in terms of the Pauli matrices, σ_i , $i = x, y, z$, the photon transverse polarisation, \vec{e}_γ , and the unit vector directed along the momentum of the initial photon $\vec{n} = \vec{p}_\gamma/|\vec{p}_\gamma|$.

In our previous studies [1, 2] (see also Ref. [18]) we assumed a simple S -wave structure of the vertex $V \rightarrow Q\bar{Q}$ (corresponding to only the first non-derivative part of expression for $\hat{\mathcal{O}}_{\gamma^*}^T$ in Eq. (2.6)) which differs from the photon-like $\gamma^* \rightarrow Q\bar{Q}$ transition with more complicated structure $\psi_\mu \bar{u} \gamma^\mu u$. The corresponding photon-like quarkonium wave function in the rest frame of the $Q\bar{Q}$ -pair, in general, besides the S -wave contains also a D -wave contribution. The weight of the latter cannot be straightforwardly obtained in the potential approach (i.e. by using any well-defined $Q\bar{Q}$ interaction potential). At the same time, it is strongly correlated with the Lorentz structure of the quarkonium $V \rightarrow Q\bar{Q}$ wave function. Nevertheless, the photon-like vector-meson wave function is used practically in all calculations in the literature so far devoted to photo-, electro- and hadroproduction of heavy quarkonia but ignoring the spin effects. For this reason, in the present paper we analyse

for the first time the effects of Melosh transformation in the case of widely-used photon-like quarkonium vertex.

So, in contrast to Refs. [1, 2] and following a frequently used convention in the literature [10, 32–34], let us now assume the same Lorentz structure of the photon $\gamma^* \rightarrow Q\bar{Q}$ and vector meson $V \rightarrow Q\bar{Q}$ transitions. Consequently, the LF wave function for the $Q\bar{Q}$ Fock component of heavy T and L polarized quarkonia in Eq. (2.1) takes the following form relying on factorization of the spatial and spin-dependent parts,

$$\Phi_{V_{T,L}}^{(\mu,\bar{\mu})}(r, z) = \frac{\sqrt{N_c}}{\sqrt{2}} \chi_Q^{\mu\dagger} \hat{O}_V^{T,L} \tilde{\chi}_Q^\mu \Psi_{V_{T,L}}(r, z), \quad \Psi_{V_{T,L}}(r, z) = \mathcal{N}_{T,L} \Psi_V(r, z), \quad (2.7)$$

where $\mathcal{N}_{T,L}$ are the normalisation factors satisfying

$$N_c \int d^2r \int dz \{ m_Q^2 |\Psi_{V_T}(\vec{r}, z)|^2 + [z^2 + (1-z)^2] |\partial_r \Psi_{V_T}(\vec{r}, z)|^2 \} = 1 \quad (2.8)$$

$$4 N_c M_V^2 \int d^2r \int dz z^2 (1-z)^2 |\Psi_{V_L}(\vec{r}, z)|^2 = 1, \quad (2.9)$$

and the operators $\hat{O}_V^{T,L}$ take a similar form as those in Eq. (2.6),

$$\begin{aligned} \hat{O}_V^T &= m_Q \vec{\sigma} \cdot \vec{e}_V + i(1-2z)(\vec{\sigma} \cdot \vec{n})(\vec{e}_V \cdot \vec{\nabla}_r) + (\vec{n} \times \vec{e}_V) \cdot \vec{\nabla}_r, \\ \hat{O}_V^L &= 2 M_V z(1-z) \vec{\sigma} \cdot \vec{n}. \end{aligned} \quad (2.10)$$

Here, \vec{e}_V is the vector meson polarization vector.

The spin rotation effects causing a transformation $\Phi_V^{(\mu,\bar{\mu})} \rightarrow \tilde{\Phi}_V^{(\mu,\bar{\mu})}$ are straightforwardly incorporated as follows. Starting from the factorised expression

$$\tilde{\Phi}_{V_{T,L}}^{(\mu,\bar{\mu})}(\vec{p}_T, z) = \sqrt{N_c} U_{T,L}^{(\mu,\bar{\mu})}(\vec{p}_T, z) \Psi_{V_{T,L}}(p_T, z), \quad (2.11)$$

where $\Psi_V(p_T, z)$ is the Fourier-image of the spatial part of the quarkonium wave function $\Psi_V(r, z)$ introduced in Eq. (2.7), such that

$$\Psi_V(r, z) = \int_0^\infty dp_T p_T J_0(p_T r) \Psi_V(p_T, z), \quad (2.12)$$

and the operators

$$U_{T,L}^{(\mu,\bar{\mu})}(\vec{p}_T, z) = \frac{1}{\sqrt{2}} \xi_Q^{\mu\dagger} \hat{O}_V^{T,L} \tilde{\xi}_Q^\mu, \quad \tilde{\xi}_Q^\mu = i\sigma_y \xi_Q^{\mu*}, \quad (2.13)$$

are written in the vector-meson rest frame in terms of quark spinors ξ connected to spinors χ in the LF frame by the following relation,

$$\xi_Q^\mu = R(\vec{p}_T, z) \chi_Q^\mu, \quad \tilde{\xi}_Q^\mu = R(-\vec{p}_T, 1-z) \chi_Q^\mu. \quad (2.14)$$

This transformation has a form of rotation in the space of spinor indices and is well-known as the Melosh spin transform (for more details, see Refs. [15, 18]). Here, the rotation matrix R is found as

$$R(\vec{p}_T, z) = \frac{m_Q + z M_V - i(\vec{\sigma} \times \vec{n}) \cdot \vec{p}_T}{\sqrt{(m_Q + z M_V)^2 + p_T^2}}. \quad (2.15)$$

Here the limit of no spin transformation, corresponding to the unit R -matrix, leads to a reduction of the expression Eq. (2.11) to Eq. (2.7) (i.e. $\tilde{\Phi} \rightarrow \Phi$).

Substituting

$$\tilde{\xi}_Q^{\bar{\mu}} = i\sigma_y R^*(-\vec{p}_T, 1-z)(-i)\sigma_y^{-1}\tilde{\chi}_Q^{\bar{\mu}}, \quad \xi_Q^{\mu\dagger} = \chi_Q^{\mu\dagger} R^\dagger(\vec{p}_T, z), \quad (2.16)$$

into Eq. (2.13) one obtains

$$U_{T,L}^{(\mu,\bar{\mu})}(\vec{p}_T, z) = \frac{1}{\sqrt{2}}\chi_Q^{\mu\dagger} R^\dagger(\vec{p}_T, z) \hat{O}_V^{T,L} \sigma_y R^*(-\vec{p}_T, 1-z)\sigma_y^{-1}\tilde{\chi}_Q^{\bar{\mu}}. \quad (2.17)$$

Consequently, the resulting dipole formula for the quarkonium electroproduction amplitude reads,

$$\text{Im}\mathcal{A}_{T,L}^{\gamma^* p \rightarrow V p}(x, Q^2) = \int_0^1 dz \int d^2r \Sigma_{T,L}(\vec{r}, z; Q^2) \sigma_{Q\bar{Q}}(x, r), \quad (2.18)$$

where

$$\Sigma_{T,L}(\vec{r}, z; Q^2) = \int \frac{d^2 p_T}{2\pi} e^{-i\vec{p}_T \vec{r}} \Psi_{V_{T,L}}(p_T, z) \sum_{\mu, \bar{\mu}} U_{T,L}^{\dagger(\mu, \bar{\mu})}(\vec{p}_T, z) \Psi_{\gamma_{T,L}^*}(r, z; Q^2). \quad (2.19)$$

Finally, and taking into account the no spin-flip contribution only, together with Eqs. (2.18) and (2.19), one arrives at the following final expressions,

$$\begin{aligned} \text{Im}\mathcal{A}_L(x, Q^2) &= Z_Q \frac{N_c \sqrt{\alpha_{em}}}{2\pi\sqrt{2}} \int_0^1 dz \int d^2r \Sigma_L(\vec{r}, z; Q^2) \sigma_{Q\bar{Q}}(x, r), \\ \Sigma_L &= 8 M_V Q z^2 (1-z)^2 K_0(\varepsilon r) \int dp_T p_T J_0(p_T r) \Psi_{V_L}(p_T, z) \frac{m_T m_L + m_Q^2}{m_Q(m_T + m_L)}, \end{aligned} \quad (2.20)$$

for a longitudinally polarized photon and quarkonium, and

$$\begin{aligned} \text{Im}\mathcal{A}_T(x, Q^2) &= Z_Q \frac{N_c \sqrt{\alpha_{em}}}{2\pi\sqrt{2}} \int_0^1 dz \int d^2r \sigma_{Q\bar{Q}}(x, r) \left[\Sigma_T^{(1)}(\vec{r}, z; Q^2) + \Sigma_T^{(2)}(\vec{r}, z; Q^2) \right], \\ \Sigma_T^{(1)} &= K_0(\varepsilon r) \int dp_T p_T J_0(p_T r) \Psi_{V_T}(p_T, z) \frac{m_Q^2(m_L^2 + 2m_L m_T + 2m_T^2) - m_L^2 m_T^2}{m_Q(m_T + m_L)}, \\ \Sigma_T^{(2)} &= K_1(\varepsilon r) \varepsilon \int dp_T p_T^2 J_1(p_T r) \Psi_{V_T}(p_T, z) \frac{m_L m_T (m_Q^2 - m_L^2)}{m_Q^3(m_T + m_L)}, \end{aligned} \quad (2.21)$$

for a transversely polarised photon and quarkonium, where

$$m_T^2 = m_Q^2 + p_T^2, \quad m_L^2 = 4m_Q^2 z(1-z), \quad (2.22)$$

such that

$$M_V^2 = \frac{m_T^2}{z(1-z)}, \quad (2.23)$$

is the meson mass squared expressed in terms of the basic kinematic variables on the LC, m_T and z .

Excluding the effects of the Melosh spin transformation, the corresponding expressions for the Σ_L and $\Sigma_T^{(1,2)}$ functions in Eqs. (2.20) and (2.21) are reduced to the following simple and standard form,

$$\Sigma_L(\vec{r}, z; Q^2) = 8 M_V Q z^2 (1-z)^2 K_0(\varepsilon r) \int dp_T p_T J_0(p_T r) \Psi_{V_L}(p_T, z), \quad (2.24)$$

and

$$\begin{aligned} \Sigma_T^{(1)}(\vec{r}, z; Q^2) &= 2 m_Q^2 K_0(\varepsilon r) \int dp_T p_T J_0(p_T r) \Psi_{V_T}(p_T, z), \\ \Sigma_T^{(2)}(\vec{r}, z; Q^2) &= 2 [z^2 + (1-z)^2] K_1(\varepsilon r) \varepsilon \int dp_T p_T^2 J_1(p_T r) \Psi_{V_T}(p_T, z). \end{aligned} \quad (2.25)$$

The spatial part of the LF quarkonium wave function (2.7), $\Psi_V(r, z)$, can be found in the framework of potential approach. As the first step, we start with determination of a quarkonia wave function $\Psi_{nlm}(\vec{\rho})$ in the $Q\bar{Q}$ rest frame. In the considering case of S -wave production, one can safely represent $\Psi_{nlm}(\vec{\rho})$ in the following factorized form,

$$\Psi_{nlm}(\vec{\rho}) = \Psi_{nl}(\rho) \cdot Y_{lm}(\theta, \varphi), \quad (2.26)$$

where functions $\Psi_{nl}(\rho)$ and $Y_{lm}(\theta, \varphi)$ are the radial and orbital parts of the wave function, respectively. The former part depends on the three-dimensional $Q\bar{Q}$ separation $\vec{\rho}$ and has been obtained by solving the Schroedinger equation for different potentials $V_{Q\bar{Q}}(\rho)$ for quark and antiquark interaction according to the formalism of Refs. [1, 2, 18]. So far, there is no unambiguous way to relate the radial wave function of the lowest Fock component $|Q\bar{Q}\rangle$ in the $Q\bar{Q}$ rest frame, $\Psi_{nl}(\rho)$, with its spatial wave function in the LF frame, $\Psi_V(r, z)$, by a simple Lorentz boost transformation. Usually, one employs a particularly simple recipe found in Ref. [35] and described in detail in Refs. [1, 2, 10, 18]. As a result, one ends up with the momentum-space spatial quarkonium wave function in the LF frame $\Psi_V(p_T, z)$ which readily enters Eqs. (2.11), (2.20) and (2.21). By Fourier transformation (2.12), one obtains the corresponding impact-parameter spatial wave function $\Psi_V(r, z)$ to be used in Eq. (2.7).

The effect of Melosh spin rotation in the total cross sections of $\gamma^* p \rightarrow J/\psi(\psi', \Upsilon, \Upsilon', \Upsilon'') p$ processes is not connected to a particular form of the interaction potential $V_{Q\bar{Q}}(\rho)$. Consequently, following Refs. [1, 2], in the present study we adopt only the following two heavy quark interaction potentials, which provide the fairly good description of the experimental data – the Buchmüller-Tye (BT) [36] and the power-like (POW) potential [37].

As was mentioned above, the essential ingredient of the production amplitude (2.1) in the dipole picture is the universal phenomenological dipole cross section $\sigma_{Q\bar{Q}}(x, r)$ that allows to describe in an uniform way various high-energy processes, both inclusive and diffractive. It represents the interaction of a $Q\bar{Q}$ dipole of a transverse separation \vec{r} with the proton target (at a given Bjorken x) and, consequently, the magnitudes of $\sigma_{Q\bar{Q}}$ at different values \vec{r} are the eigenvalues of the elastic amplitude operator. Due to flavor universality of the QCD coupling, the dipole cross section is also typically considered to be flavor-independent, to a good accuracy. Another pronounced feature is known as the color transparency: $\sigma_{Q\bar{Q}}(r) \propto r^2$ for $r \rightarrow 0$.

So far, the dipole cross section cannot be predicted reliably from the first principles due to poorly known higher-order pQCD corrections and nonperturbative effects. Therefore,

we are obliged to use only its phenomenological parametrizations obtained from the fit of the high-precision DIS data available from HERA collider. Although about ten different parametrizations for $\sigma_{Q\bar{Q}}(x, r)$ can be found in the literature, for our purposes here we use only two of them following the results of Ref. [1]. The first, simplest but phenomenologically very successful parametrization conventionally denoted as GBW has been suggested in Ref. [38]. The second parametrization denoted as KST has been proposed in Ref. [39]. A more detailed description of both models can be found in Ref. [1] and will not be repeated further on in this work.

As was already emphasized in Ref. [1], one can treat the variations in predictions based upon the GBW [38] and KST [39] models for the dipole cross section as a good measure of the underlined theoretical uncertainties. Another choice among the available dipole parametrizations has practically no impact on conclusions of this work that concern the relative onset of spin rotation effects in exclusive photo- and electroproduction of heavy quarkonia.

III. MODEL PREDICTIONS VS DATA

As was mentioned above, in the present paper we follow the common trend in the literature devoted to studies of exclusive quarkonia electroproduction (see e.g. Refs. [9–11, 32–34, 40]) and assume the same Lorentz structure of $V \rightarrow Q\bar{Q}$ and $\gamma^* \rightarrow Q\bar{Q}$ wave functions. As was thoroughly described in the previous section, the calculations of the exclusive quarkonia electroproduction cross sections are performed in the framework of color dipole approach. Besides, we incorporate also the effects of Melosh spin rotation representing the transformation of the spin-dependent components of the quarkonium wave function from the meson rest frame to the LF frame. Such analysis of the spin effects is performed here for the first time treating the photon-like structure of the $V \rightarrow Q\bar{Q}$ vertex and is complementary to our previous studies [1, 2] employing a different (S -wave only) and more simple structure of the vector-meson LF wave function. The corresponding numerical results have been obtained using Eq. (2.2) with amplitudes (2.21), (2.20).

In Figs. 1 and 2 we present the results for the total cross sections of $\gamma^* p \rightarrow J/\psi p$ (upper panels) and $\gamma^* p \rightarrow \psi' p$ (lower panels) processes. The cross sections for $J/\psi(1S)$ production are shown together with the available data as functions of γp collision energy W and the hard scale of the process, $Q^2 + M_{J/\psi}^2$. These calculations were performed by using the KST and GBW dipole parametrizations as shown by thin and thick lines, respectively.

Both Figs. 1 and 2 clearly demonstrate a good agreement of the results with the available data when one excludes the spin rotation effects from consideration, what is the current situation in the literature. However, the Melosh spin transformation leads to a significant 20 – 30 % reduction of the photoproduction cross section for the $1S$ charmonium spoiling such a good description of the data. This is a keystone result that raises the basic question about the correctness of the conventional predictions, being frequently presented in the literature that apparently rely on an unjustified assumption about a photon-like structure of the vector-meson wave function and ignoring the spin effects.

Here, we would like to emphasize that the magnitude of spin effects is correlated with a structure of the $V \rightarrow Q\bar{Q}$ transition. In our previous studies [1, 2], treating a simple non-photon-like structure of the vector meson LF wave functions (i.e. considering only the S -wave component of the quarkonium wave function in the rest-frame of the $Q\bar{Q}$ fluctuation), the Melosh spin transformation causes a significant enhancement of the photoproduction cross section. Such a behavior is radically different from the photon-like $V \rightarrow Q\bar{Q}$ transition.

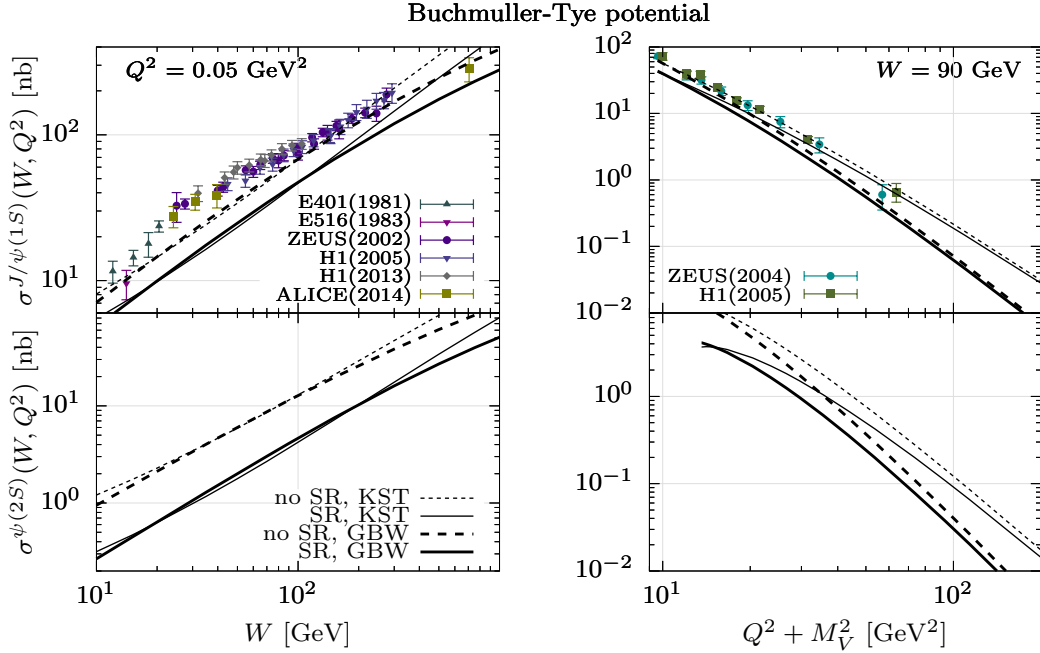


FIG. 1: **Left panels:** Cross sections $\gamma p \rightarrow J/\psi(1S)p$ (left upper panel) and $\gamma p \rightarrow \psi'(2S)p$ (left lower panel) processes with $Q^2 = 0.05 \text{ GeV}^2$ as functions of γp collision c.m. energy W (the experimental data are from Refs. [41–46]). **Right panels:** The same cross sections but as functions of the scale $Q^2 + M_{J/\psi}^2$ of the $J/\psi(1S)$ production process (right upper box) and $Q^2 + M_{\psi'}^2$ of the $\psi'(12S)$ production process (right lower box) at fixed $W = 90 \text{ GeV}$ (the data are from Refs. [44, 47]). Our results have been obtained using the wave functions of $J/\psi(1S)$ and $\psi'(2S)$ mesons generated by the Buchmüller-Tye potential [36]. The results with and without the Melosh spin transform are indicated by solid and dashed lines, respectively. Thin and thick lines represent the results obtained with KST [39] and GBW [38] dipole parameterisations, respectively.

Namely, in the latter case the Melosh rotation leads to a significant reduction of the cross section instead as is demonstrated in left panels of Figs. 1 and 2. We notice that the spin effects continuously disappear at large Q^2 as is demonstrated in Figs. 1 and 2 (right panels).

Note that in recent theoretical studies of heavy quarkonia produced in ultra-peripheral collisions at RHIC and the LHC a similar structure of both $V \rightarrow Q\bar{Q}$ and $\gamma^* \rightarrow Q\bar{Q}$ transitions is imposed while the effects of the Melosh spin transformation are ignored (see Ref. [2] and references therein). As was demonstrated above, this way leads to a good overall description of the data which creates a very peculiar situation when two wrong assumptions (the photon-like structure of the $V \rightarrow Q\bar{Q}$ vertex and the absence of spin rotation effects) may cause mutually compensating effects. Indeed, Figs. 1 and 2 show that spin effects spoil such a successful description of data and this may represent the reason why they are neglected in the most of recent papers. A more physically justified approach of Refs. [1, 2] that does not invoke any of these two wrong assumptions lead to as good description of the data as the conventional results in the literature. This poses the natural and physically critical question about the significance of the D -wave contribution to the production amplitude which is effectively included in the case of a photon-like vector-meson wave function.

The nodal structure of the wave function for the radially excited $\psi'(2S)$ state enhances

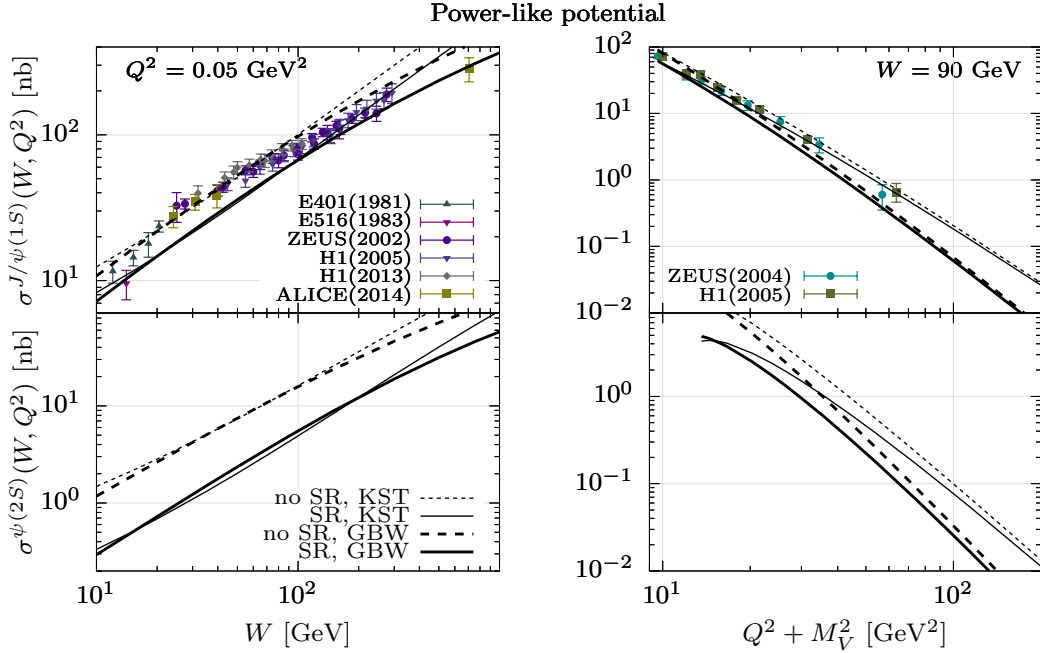


FIG. 2: The same as Fig. 1, except using the $J/\psi(1S)$ and $\psi'(2S)$ radial wave functions computed with the power-like $Q\bar{Q}$ potential [37].

the onset of spin rotation effects that are much stronger compared to $J/\psi(1S)$ production reducing the cross section by above a factor of $2 \div 3$ as is demonstrated in lower panels of Figs. 1 and 2.

As was already mentioned in Sect. I and also discussed in Ref. [1] the scanning radius given by Eq. (1.1) controls the universality between different cross sections. Consequently, one should expect the same magnitude of electroproduction cross sections as well as the same onset of spin effects for $\gamma^* p \rightarrow J/\psi(1S) p$ process at some scale $Q^2(J/\psi)$, and for $\Upsilon(1S)$ photoproduction. Such value $Q^2(J/\psi) \sim 130 \div 140 \text{ GeV}^2$ has been estimated in Ref. [1] from Eq. (1.1).

The both Figs. 1 and 2 demonstrate a gradual disappearance of the spin rotation effects with Q^2 and their very weak onset at large scale $Q^2(J/\psi)$. Thus, following the scanning phenomenon, one expects such a weak onset of spin effects also in $\Upsilon(1S)$ photoproduction as is shown in Figs. 3 and 4 for the Buchmüller-Tye and power-law potentials, respectively. The results are also given for the energy and scale dependencies of the elastic (real and virtual) photoproduction cross sections for radially excited bottomonia states $\Upsilon'(2S)$ and $\Upsilon''(3S)$. The existence of the node in their radial wave functions leads to a stronger onset of spin effects compared to production of the $\Upsilon(1S)$ state.

In comparison with real photoproduction of $J/\psi(1S)$ a weak onset of the Melosh spin transformation in photoproduction of $\Upsilon(1S)$ does not spoil an agreement with available data as is shown in upper left panels of Figs. 3 and 4. A rough measure of theoretical uncertainties is indicated by typical differences in numerical results corresponding to the GBW and KST dipole parametrizations.

Indeed, as was concluded previously in Refs. [1, 2] treating the case of a different structure for $\gamma^* \rightarrow Q\bar{Q}$ and $V \rightarrow Q\bar{Q}$ transitions and now analyzing the case of a similar structure

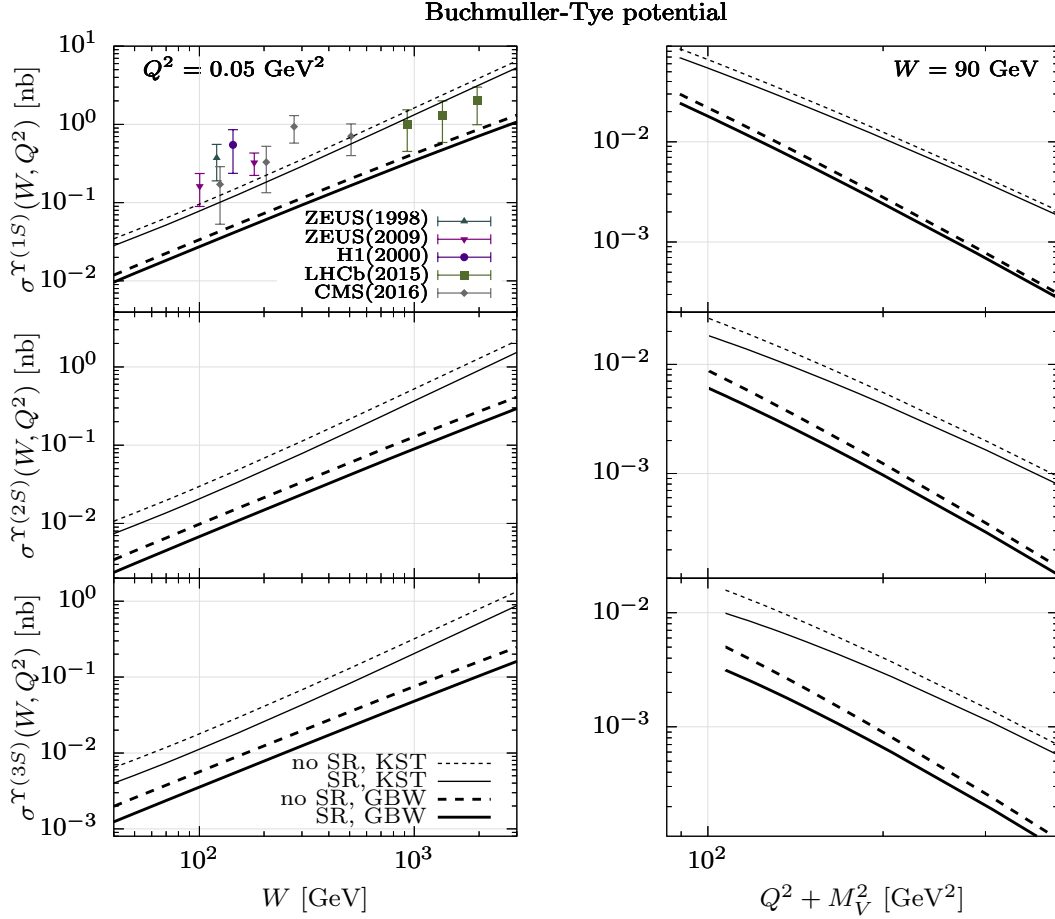


FIG. 3: The same as Fig. 1 but for $\Upsilon(1S)$ (upper panels), $\Upsilon'(2S)$ (middle panels) and $\Upsilon''(3S)$ (lower panels) states photoproduction (the experimental data for $\gamma p \rightarrow \Upsilon p$ process are from Ref. [25, 48–51]). Here, the radial wave functions of $\Upsilon(1S)$, $\Upsilon'(2S)$ and $\Upsilon''(3S)$ states are obtained with the Buchmüller-Tye potential [36].

of both vertices, the spin rotation effects have a huge impact on the magnitude of elastic photoproduction cross section of the processes $\gamma^* p \rightarrow J/\psi(1S) p$ resp. $\gamma^* p \rightarrow \psi'(2S) p$. While in the former case they enhance the $J/\psi(1S)$ cross section by a factor of $1.2 \div 1.3$, in the latter case they cause its $\sim 20 \div 30\%$ reduction. The nodal structure of the radially-excited wave functions causes a much stronger onset of the spin effects in photoproduction of $\psi'(2S)$ state increasing or decreasing the corresponding cross section by a factor of $2 \div 3$ depending on the structure of the quarkonium $V \rightarrow Q\bar{Q}$ transition.

Such a dramatic impact of the spin rotation can be also observed by investigating the ratio R of $\psi'(2S)$ to $J/\psi(1S)$ cross sections shown in Figs. 5 and 6 as functions of c.m. energy W and Q^2 . One notices a significant reduction of the ratio $R(Q^2 \rightarrow 0)$ due to a combination of the Melosh spin transformation with the nodal structure of the radial $\psi'(2S)$ wave function. Indeed, the ratio R is much better observable to probe the spin rotation effects than the standard cross sections since it allows to cancel out many uncertainties that are discussed in Ref. [2]. Here again, the both Figs. 5 and 6 demonstrate a reasonable accordance of our results with the available data as long as one ignores the spin rotation

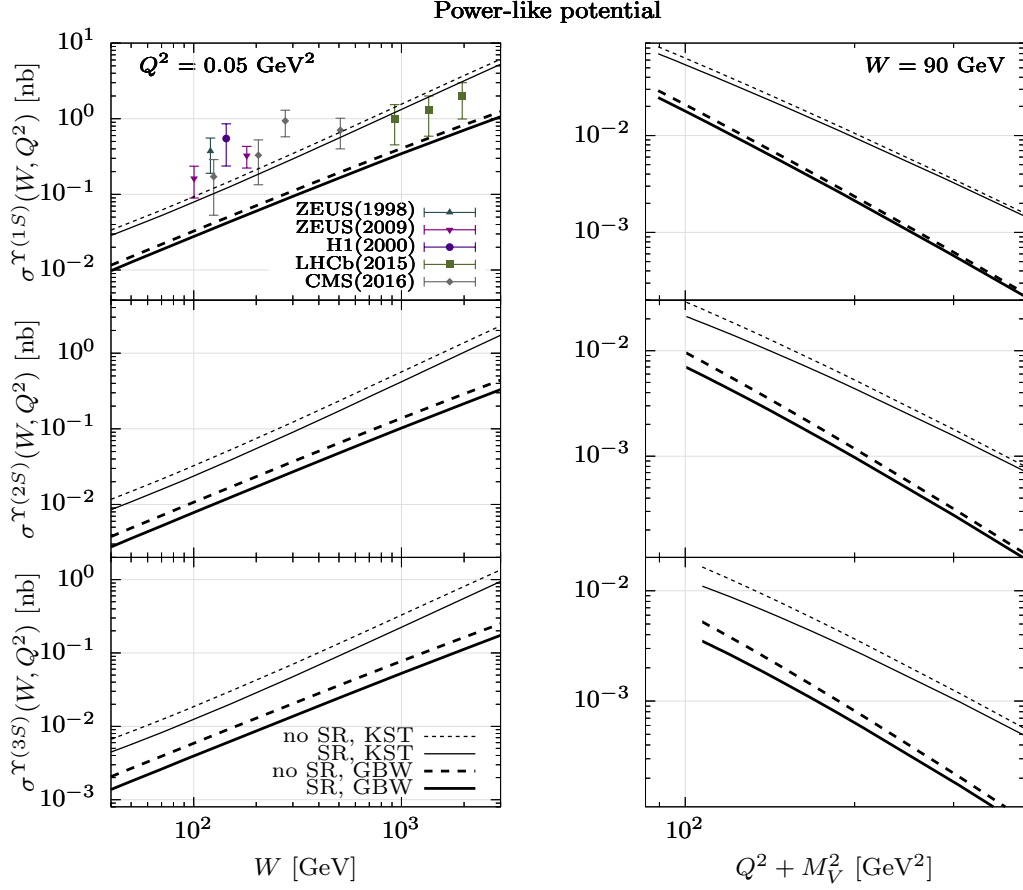


FIG. 4: The same as Fig. 3, except using the $\Upsilon(1S)$, $\Upsilon'(2S)$ and $\Upsilon''(3S)$ radial wave functions computed with the power-like $Q\bar{Q}$ potential [37].

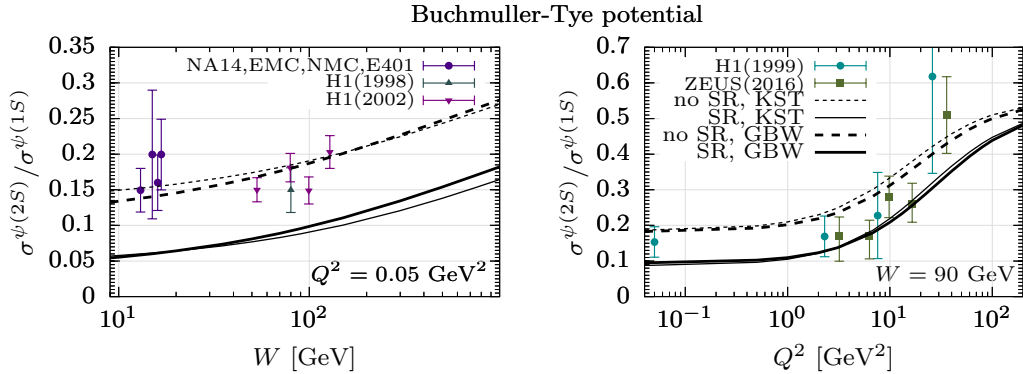


FIG. 5: **Left panel:** The $\psi'(2S)$ -to- $J/\psi(1S)$ cross sections ratio as a function γp collision c.m. energy W and with fixed $Q^2 = 0.05 \text{ GeV}^2$ (left panel), **Right panel:** The same quantity but as a function of Q^2 at fixed $W = 90 \text{ GeV}$. The results are compared to the experimental data taken from Refs. [52–59]. For more details, see the caption of Fig. 1 and the corresponding description in the text.

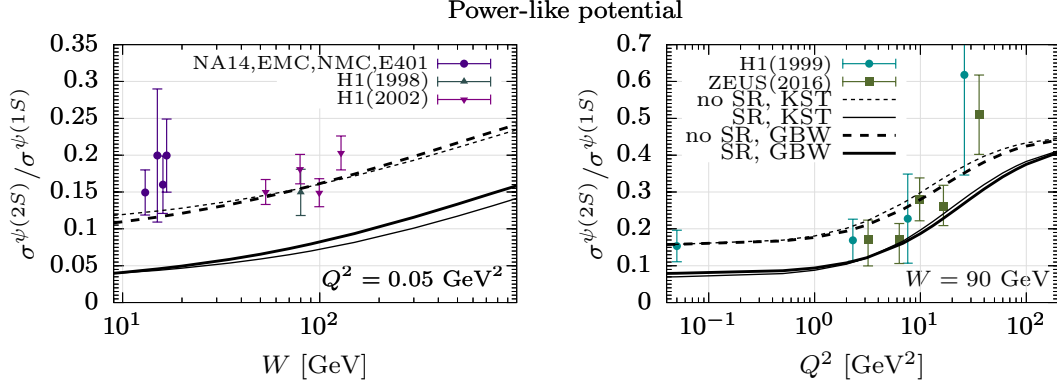


FIG. 6: The same as Fig. 5, except using the $J/\psi(1S)$ and $\psi'(2S)$ radial wave functions computed with the power-like $Q\bar{Q}$ potential [37].

effects. The onset of the Melosh transformation in the considering case of the photon-like structure of the charmonium wave function spoils significantly such an agreement .

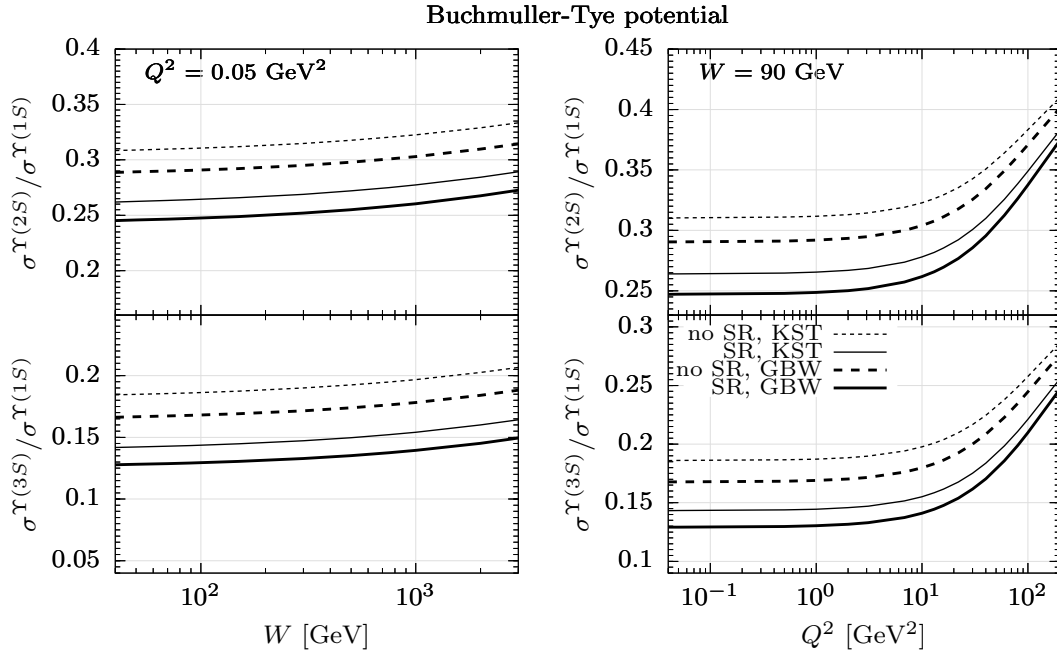


FIG. 7: The same as in Fig. 5 but for $\Upsilon'(2S)$ -to- $\Upsilon(1S)$ (upper panels) and $\Upsilon''(3S)$ -to- $\Upsilon(1S)$ (lower panels) cross sections ratio obtained using the Buchmüller-Tye potential [36].

Finally, Figs. 7 and 8 show the predictions for $\Upsilon'(2S)$ -to- $\Upsilon(1S)$ and $\Upsilon''(3S)$ -to- $\Upsilon(1S)$ ratios of photo- and electroproduction cross sections as functions of c.m. energy W and photon virtuality Q^2 . The BT and POW potentials have been used. Following the scanning phenomenon, the larger scale $Q^2 + M_V^2$ leads to a smaller scanning radius, Eq. (1.1) and, consequently, to a smaller $Q\bar{Q}$ dipole sizes thus reducing the onset of spin rotation effects. However, a larger size of radially-excited bottomonia compared to that of $\Upsilon(1S)$ state naturally leads to a stronger spin effect. The latter reduces more significantly the magnitude of the

ratios $\sigma(\gamma^* p \rightarrow \Upsilon'(2S) p)/\sigma(\gamma^* p \rightarrow \Upsilon(1S) p)$ and $\sigma(\gamma^* p \rightarrow \Upsilon''(3S) p)/\sigma(\gamma^* p \rightarrow \Upsilon(1S) p)$.

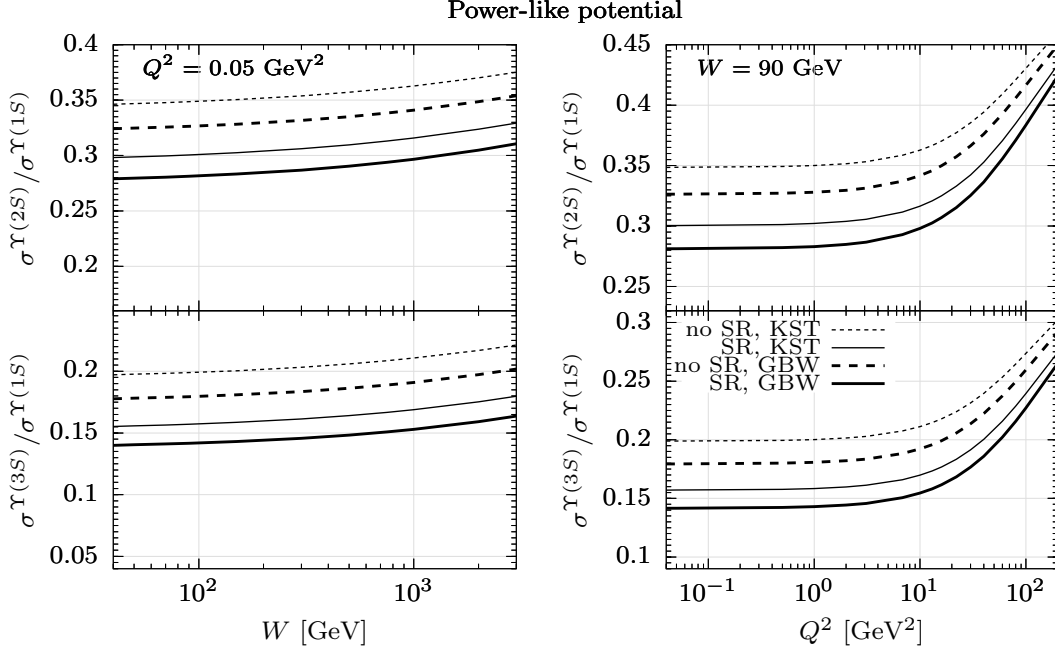


FIG. 8: The same as Fig. 7, except using the $\Upsilon(1S)$, $\Upsilon'(2S)$ and $\Upsilon''(3S)$ radial wave functions computed with the power-like $Q\bar{Q}$ potential [37].

IV. CONCLUSIONS

The present analysis represents a natural continuation of our previous studies [1, 2] of the Melosh spin transformation in elastic electroproduction of S -wave heavy quarkonia, $\gamma^* p \rightarrow V p$, where the following quarkonia states $V = J/\psi(1S), \psi'(2S), \Upsilon(1S), \Upsilon'(2S)$ and $\Upsilon''(3S)$ have been considered. In Refs. [1, 2], we have used a specific structure of the quarkonium wave function corresponding to “ S -wave-only” contribution in the $Q\bar{Q}$ rest frame. In this work, we have derived for the first time the formula (2.2) with amplitudes (2.21) and (2.20) for electroproduction of T and L polarized quarkonia including the spin rotation effects in the case of widely-used photon-like structure of the $V \rightarrow Q\bar{Q}$ light-front wave function. When transformed to the quarkonium rest frame, the latter contains an unknown D -wave term and thus has unclear prospects as it cannot be consistently obtained in a potential approach starting from an interquark potential whereas a detailed analysis of D -wave contribution and its phenomenological implications is still missing in the literature. Our current study is thus complementary to our previous analysis [1, 2] indirectly showing an interplay of the Lorentz structure of the quarkonium transition vertex and the Melosh spin rotation.

Although the assumption about a similar structure of both $\gamma^* \rightarrow Q\bar{Q}$ and $V \rightarrow Q\bar{Q}$ transitions is not well justified, it is frequently employed in the current literature. Moreover, the effects of Melosh spin transformation are usually ignored in the corresponding calculations, what in practice leads to a biased interpretation of various underlined phenomena which

may occur in electroproduction of heavy quarkonia, on top of other theoretical uncertainties studied earlier in Refs. [1, 2].

In order to compute the electroproduction cross section for heavy quarkonia using the dipole model representation for the factorized light-cone transversely (2.21) and longitudinally (2.20) polarized production amplitudes, one needs to correctly identify several important ingredients. One such ingredient is the light-front photon wave function for the leading-order Fock $\gamma^* \rightarrow Q\bar{Q}$ fluctuation, another is the light-front vector meson wave function $\Psi_V(r, z)$ for the S -wave heavy quarkonium, and, finally, the universal dipole cross section $\sigma_{Q\bar{Q}}(x, r)$.

The light-front photon wave function is well-known without any significant uncertainties. However, in order to obtain the heavy quarkonium wave functions in the light-front (or infinite-momentum) frame starting from a NRQCD wave function in the rest frame of $Q\bar{Q}$ -pair we use a popular prescription suggested by Terent'ev in Ref. [35]. The corresponding nonrelativistic wave functions found by solving the Schroedinger equation for two different realistic heavy-quark interaction potentials – the Buchmüller-Tye [36] and power-like [37] models. For the dipole cross section $\sigma_{Q\bar{Q}}(x, r)$ as a reference we adopted two distinct KST [39] and GBW [38] parametrizations. Our predictions have been obtained including the effects of Melosh spin transformation [15] responsible for the transition of the spin-orbital part of quarkonium wave functions from the $Q\bar{Q}$ rest frame to the light-front frame imposing a similar structure for the $\gamma^* \rightarrow Q\bar{Q}$ and $V \rightarrow Q\bar{Q}$ transitions.

Our observations are the following.

- (i) The onset of spin rotation effects is strongly correlated with a structure of the quarkonium vertex. As was shown in our previous analyses [1, 2] based on a distinct structure of the $V \rightarrow Q\bar{Q}$ and $\gamma^* \rightarrow Q\bar{Q}$ wave functions, the Melosh transformation enhances substantially the magnitude of corresponding photo- and electroproduction cross sections. However, in the case of a photon-like $V \rightarrow Q\bar{Q}$ wave function the spin effects cause a notable reduction of quarkonium production yields thus spoiling a reasonable agreement with the experimental data. Consequently, since the Melosh spin transformation must actually be included in such calculations, our negative result raises the question about the true structure of the quarkonium wave function. One may conclude that the standard assumption about the photon-like structure of the quarkonium $Q\bar{Q}$ fluctuation, frequently used in the literature without any justification, should be revised. This conclusion has a potentially big impact on interpretations of various phenomena emerging in recent studies of quarkonium production in ultra-peripheral collisions at RHIC and the LHC.
- (ii) The scanning phenomenon, represented by Eq. (1.1), leads to universal properties in production of various quarkonia states. Consequently, we found that the spin effects are very similar in the charmonia and bottomonia cross sections at a fixed value of the hard scale $Q^2 + M_V^2$.
- (iii) The onset of spin effects is stronger in production of radially excited quarkonia due to a nodal structure of corresponding radial wave functions. In the case of $\psi'(2S)$ production, the Melosh transformation leads to a reduction of the production cross section by a factor of $2 \div 3$ causing also a notable decrease of the $\psi'(2S)$ -to- $J/\psi(1S)$ ratio of the cross sections, therefore spoiling an agreement with the available experimental data. This observation is opposite to the result of Refs. [1, 2] using a different, non-photon-like (manifestly, S -wave) $V \rightarrow Q\bar{Q}$ wave function, when the spin effects cause a substantial enhancement of the corresponding $\psi'(2S)$ -to- $J/\psi(1S)$ ratio improving an agreement with the data. Again, such a result stimulates the question about the correct structure of the heavy quarkonium wave

functions.

(iv) In the case of $J/\psi(1S)$ electroproduction, the spin rotation effects get gradually reduced with Q^2 , and according to the scanning phenomenon we find a rather weak onset of these effects as well as in photoproduction of the $\Upsilon(1S)$ state.

(v) The nodal structure of the radial wave function for $\Upsilon'(2S)$ and $\Upsilon''(3S)$ states leads to a stronger onset of the spin rotation effects than that in electroproduction of $1S$ bottomonia.

In summary, an underestimation of the importance of the Melosh spin transformation in photo- and electroproduction of heavy quarkonia may lead to a temptation to incorporate other effects in order to obtain a better agreement with the data. For example, the photon-like structure of the quarkonium vertex has been conventionally chosen as the one that leads to viable predictions when compared to the HERA data and thus is frequently used in the ongoing studies (see e.g. Ref. [2] and references therein). However, this is done without any physical justification, and on top of that ignoring the spin rotation effects. The latter indeed spoil a good agreement with the data when combined with a photon-like quarkonium wave function, as one of the main results of our current work. This result therefore calls for cautiousness in making conclusions and physics interpretations of many recent results in the literature. Finally, it is worth mentioning that more precise data on quarkonium production in ultra-peripheral and heavy-ion collisions at RHIC and the LHC are certainly needed for a better understanding of the quarkonium formation dynamics. Moreover, the planned measurements at the future electron-ion collider may shed more light on the onset of spin effects which can be considered as an important new probe for the underlying structure of the quarkonium wave function.

Acknowledgements

J.N. work was partially supported by grants LTC17038 and LTT18002 of the Ministry of Education, Youth and Sports of the Czech Republic, by the project of the European Regional Development Fund CZ02.1.01/0.0/0.0/16.019/0000778, and by the Slovak Funding Agency, Grant 2/0007/18. R.P. is supported in part by the Swedish Research Council grants, contract numbers 621-2013-4287 and 2016-05996, by the Ministry of Education, Youth and Sports of the Czech Republic, project LT17018, as well as by the European Research Council (ERC) under the European Union's Horizon 2020 research and innovation programme (grant agreement No 668679). The work of M.K. was supported in part by the Conicyt Fondecyt grant Postdoctorado N.3180085 (Chile) and by the grant LTC17038 of the Ministry of Education, Youth and Sports of the Czech Republic. The work has been performed in the framework of COST Action CA15213 "Theory of hot matter and relativistic heavy-ion collisions" (THOR).

-
- [1] M. Krelina, J. Nemchik, R. Pasechnik and J. Cepila; *Eur. Phys.J.* **C79**, 154 (2019).
 - [2] J. Cepila, J. Nemchik, M. Krelina and R. Pasechnik; *Eur. Phys.J.* **C79**, 495 (2019).
 - [3] I.P. Ivanov, N.N. Nikolaev and A.A. Savin; *Phys. Part. Nucl.* **37**, 1 (2006).
 - [4] N. Brambilla *et al.* [Quarkonium Working Group], **hep-ph/0412158**.
 - [5] N. Brambilla *et al.*; *Eur. Phys. J.* **C71**, 1534 (2011).
 - [6] T. Matsui and H. Satz; *Phys. Lett.* **B178**, 416 (1986).

- [7] B.Z. Kopeliovich, J. Nemchik, N.N. Nikolaev, B.G. Zakharov; Phys. Lett. **B309**, 179 (1993).
- [8] B.Z. Kopeliovich, J. Nemchik, N.N. Nikolaev, B.G. Zakharov; Phys. Lett. **B324**, 469 (1994).
- [9] J. Nemchik, N.N. Nikolaev, B.G. Zakharov; Phys. Lett. **B341**, 228 (1994).
- [10] J. Nemchik, N.N. Nikolaev, E. Predazzi, B.G. Zakharov; Z. Phys. **C75**, 71 (1997).
- [11] B.Z. Kopeliovich, J. Nemchik, A. Schafer and A.V. Tarasov; Phys. Rev. **C65**, 035201 (2002).
- [12] B.Z. Kopeliovich, J. Nemchik and I. Schmidt; Phys. Rev. **C76**, 025210 (2007).
- [13] B.Z. Kopeliovich and B. Povh; J. Phys. **G30**, S999 (2004).
- [14] B.Z. Kopeliovich, B. Povh and I. Schmidt; Nucl. Phys. **A782**, 24 (2007).
- [15] H.J. Melosh; Phys. Rev. **D9**, 1095 (1974).
- [16] B.Z. Kopeliovich and B.G. Zakharov; Phys. Rev. **D44**, 3466 (1991).
- [17] J. Nemchik, N.N. Nikolaev and B.G. Zakharov; Phys. Lett. **B339**, 194 (1994).
- [18] J. Hufner, Y.P. Ivanov, B.Z. Kopeliovich and A.V. Tarasov; Phys. Rev. **D62**, 094022 (2000).
- [19] J. Nemchik; Phys. Rev. **D63**, 074007 (2001).
- [20] J. Nemchik; Eur. Phys. J. **C18**, 711 (2001).
- [21] I. Babiarz, V. P. Goncalves, R. Pasechnik, W. Schäfer and A. Szczurek, Phys. Rev. **D100**, 054018 (2019).
- [22] I. P. Ivanov, arXiv:[hep-ph/9909394](https://arxiv.org/abs/hep-ph/9909394).
- [23] A. B. Zamolodchikov, B. Z. Kopeliovich and L.I. Lapidus; JETP Lett. **33**, 595 (1981).
- [24] M.G. Ryskin, R.G. Roberts, A.D. Martin and E.M. Levin; Z. Phys. **C76**, 231 (1997).
- [25] C. Adloff *et al.* [H1 Collaboration]; Phys. Lett. **B483**, 23 (2000).
- [26] J.B. Bronzan, G.L. Kane and U.P. Sukhatme; Phys. Lett. **B49**, 272 (1974).
- [27] J.R. Forshaw, R. Sandapen and G. Shaw; Phys. Rev. **D69**, 094013 (2004).
- [28] J.B. Kogut and D.E. Soper; Phys. Rev. **D1**, 2901 (1970).
- [29] J.M. Bjorken, J.B. Kogut and D.E. Soper; Phys. Rev. **D3**, 1382 (1971).
- [30] N.N. Nikolaev and B.G. Zakharov; Z. Phys. **C49**, 607 (1991).
- [31] B.Z. Kopeliovich, J. Raufeisen, A.V. Tarasov and M.B. Johnson; Phys. Rev. **C67**, 014903 (2003).
- [32] M.G. Ryskin; Z. Phys. **C57**, 89 (1993).
- [33] S.J. Brodsky, L. Frankfurt, J.F. Gunion, A.H. Mueller and M. Strikman; Phys. Rev. **D50**, 3134 (1994).
- [34] L. Frankfurt, W. Koepf and M. Strikman; Phys. Rev. **D54**, 3194 (1996).
- [35] M.V. Terentev; Sov. J. Nucl. Phys. **24**, 106 (1976) [Yad. Fiz. **24**, 207 (1976)].
- [36] W. Buchmuller and S.H.H. Tye; Phys. Rev. **D24**, 132 (1981).
- [37] N. Barik and S.N. Jena; Phys. Lett. **B97**, 265 (1980).
- [38] K. Golec-Biernat and M. Wüsthoff; Phys. Rev. **D53**, 014017 (1999).
- [39] B.Z. Kopeliovich, A. Schäfer and A.V. Tarasov; Phys. Rev. **D62**, 054022 (2000).
- [40] J. Nemchik, N.N. Nikolaev, E. Predazzi, B.G. Zakharov and V.R. Zoller; J. Exp. Theor. Phys. **86**, 1054 (1998).
- [41] M.E. Binkley *et al.* [E401 Collaboration]; Phys. Rev. Lett. **48**, 73 (1982).
- [42] B.H. Denby *et al.* [E516 Collaboration]; Phys. Rev. Lett. **52**, 795 (1984).
- [43] S. Chekanov *et al.* [ZEUS Collaboration]; Eur. Phys. J. **C24**, 345 (2002).
- [44] A. Aktas *et al.* [H1 Collaboration]; Eur. Phys. J. **C46**, 585 (2006).
- [45] C. Alexa *et al.* [H1 Collaboration]; Eur. Phys. J. **C73**, 2466 (2013).
- [46] B.B. Abelev *et al.* [ALICE Collaboration]; Phys. Rev. Lett. **113**, 232504 (2014).
- [47] S. Chekanov *et al.* [ZEUS Collaboration]; Nucl. Phys. **B695**, 3 (2004).
- [48] J. Breitweg *et al.* [ZEUS Collaboration]; Phys. Lett. **B437**, 432 (1998).

- [49] S. Chekanov *et al.* [ZEUS Collaboration]; Phys. Lett. B**680**, 4 (2009).
- [50] R. Aaij *et al.* [LHCb Collaboration]; JHEP **1509**, 084 (2015).
- [51] R. Chudasama *et al.* [CMS Collaboration]; PoS ICPAQGP **2015**, 042 (2017); arXiv:**1607.00786** [hep-ex].
- [52] R. Barate *et al.* [NA14 Collaboration]; Z. Phys. C**33**, 505 (1987).
- [53] J.J. Aubert *et al.* [EMC Collaboration]; Nucl. Phys. B**213**, 1 (1983).
- [54] P. Amaudraz *et al.* [NMC Collaboration]; Nucl. Phys. B**371**, 553 (1992).
- [55] M. Binkley *et al.* [E401 Collaboration]; Phys. Rev. Lett. **50**, 302 (1983).
- [56] C. Adloff *et al.* [H1 Collaboration]; Phys. Lett. B**421**, 385 (1998).
- [57] C. Adloff *et al.* [H1 Collaboration]; Phys. Lett. B**541**, 251 (2002).
- [58] C. Adloff *et al.* [H1 Collaboration]; Eur. Phys. J. C**10**, 373 (1999).
- [59] H. Abramowicz *et al.* [ZEUS Collaboration]; Nucl. Phys. B**909**, 934 (2016).